

Hsp16.3ΔC4, a C-terminal truncated mutant, confers strong cellular and humoral immunity against pulmonary tuberculosis

Subhasish Prusty ^{1,5,#}, Subhashree Barik ^{2,#}, Sourya Prakash Nayak ¹, R. Divya ^{1,5}, Deepak Jena ^{1,3}, Kaushik Sen ^{1,5}, Alok Kumar Panda ^{2,6}, Pooja Mahajan ⁴, Chayan Mukherjee ^{1,5}, Shaktiprasad Mishra ¹, Sakshi Priyadarsini Dutta ², Mamuni Swain ¹, Ashis Biswas ^{2,*}, Sunil Kumar Raghav ^{1,*}

¹Immuno-genomics & Systems Biology Laboratory, BRIC-Institute of Life Sciences (ILS), Bhubaneswar, India

²School of Basic Sciences, Indian Institute of Technology Bhubaneswar, Bhubaneswar, India

³School of Biotechnology, Kalinga Institute of Industrial Technology (KIIT), Bhubaneswar, India

⁴School of life sciences, Jawaharlal Nehru University (JNU), New Delhi, India

⁵Regional Centre for Biotechnology, Faridabad, India

⁶Present address: Environmental Science Laboratory, School of Applied Sciences, Kalinga Institute of Industrial Technology, Deemed to be University, Bhubaneswar, India

[#]These authors contributed equally

***Corresponding authors:**

Dr. Sunil Kumar Raghav: sunilraghav@ils.res.in

Dr. Ashis Biswas: abiswas@iitbbs.ac.in

Primary corresponding author contact email: sunilraghav@ils.res.in

Supplementary appendix

Table of content

Supplementary Table 1.....	3
Supplementary Table 2.....	4
Supplementary Table 3.....	5
Methods.....	6
Supplementary Fig. 1.....	8
Supplementary Fig. 2.....	10
Supplementary Fig. 3.....	12
Supplementary Fig. 4.....	14
Supplementary Fig. 5.....	15
Supplementary Fig. 6.....	17
Supplementary Fig. 7.....	18
Supplementary Fig. 8.....	19
Reference(s).....	20

Supplementary Table 1: List of plasmids, bacterial strains and cell line used in the study

Plasmids/Strains	Description	Source
<i>M. tuberculosis</i> H37Rv	<i>M. tuberculosis</i> laboratory strain	ATCC
BCG	Pasteur strain	A kind gift from Dr. Dhiraj Kumar
THP-1	Human monocyte cell line	NCCS, Pune
pET28b vector	Expression vector	Novagen, EMD (Gibbstown, NJ, USA)

Supplementary Table 2: List of primers used in the study

Proteins	Forward primer (5'-3')	Reverse primer (5'-3')
Hsp16.3WT	GGG AAT TCC ATA TGG CCA CCA CCC TTC	CCG CTC GAG TCA GTT GGT GGA CCG GAT C
Hsp16.3ΔC3	GGG AAT TCC ATA TGG CCA CCA CCC TTC	CCG CTC GAG TCA CCG GAT CTG AAT GTG C
Hsp16.3ΔC4	GGG AAT TCC ATA TGG CCA CCA CCC TTC	CCG CTC GAG TCA GAT CTG AAT GTG CTT TTC GG
Hsp16.3ΔC8	GGG AAT TCC ATA TGG CCA CCA CCC TTC	CCG CTC GAG TCA CTT TTC GGT TGG CTT CCC TTC
Hsp16.3ΔC12	GGG AAT TCC ATA TGG CCA CCA CCC TTC	CCG CTC GAG TCA CTT CCC TTC CGA AAC CGC CA

Supplementary Table 3: List of various antibodies and dyes used for immune studies

Mouse antibody	Fluorochrome used
Viability	Zombie UV
CD45	eFluor 506/BUV496
CD3	PE-Cy5
CD4	Alexa Fluor 700
CD8	APC-Cy7
CD62L	PE-eFluor 610
CD44	eFluor 450
CD69	Spark NIR 685
CCR7	APC
IFN- γ	PE/ PE-eFluor 610
TNF- α	BV510
IL-2	BV785
IL-4	BV711
IL-17A	BV650/APC
IL-10	BV605
CD27	FITC
CD45R/B220	eFluor 450
CD19	eFlour 780

Method:

Overexpression and purification of wild-type and C-terminal region-truncated mutants

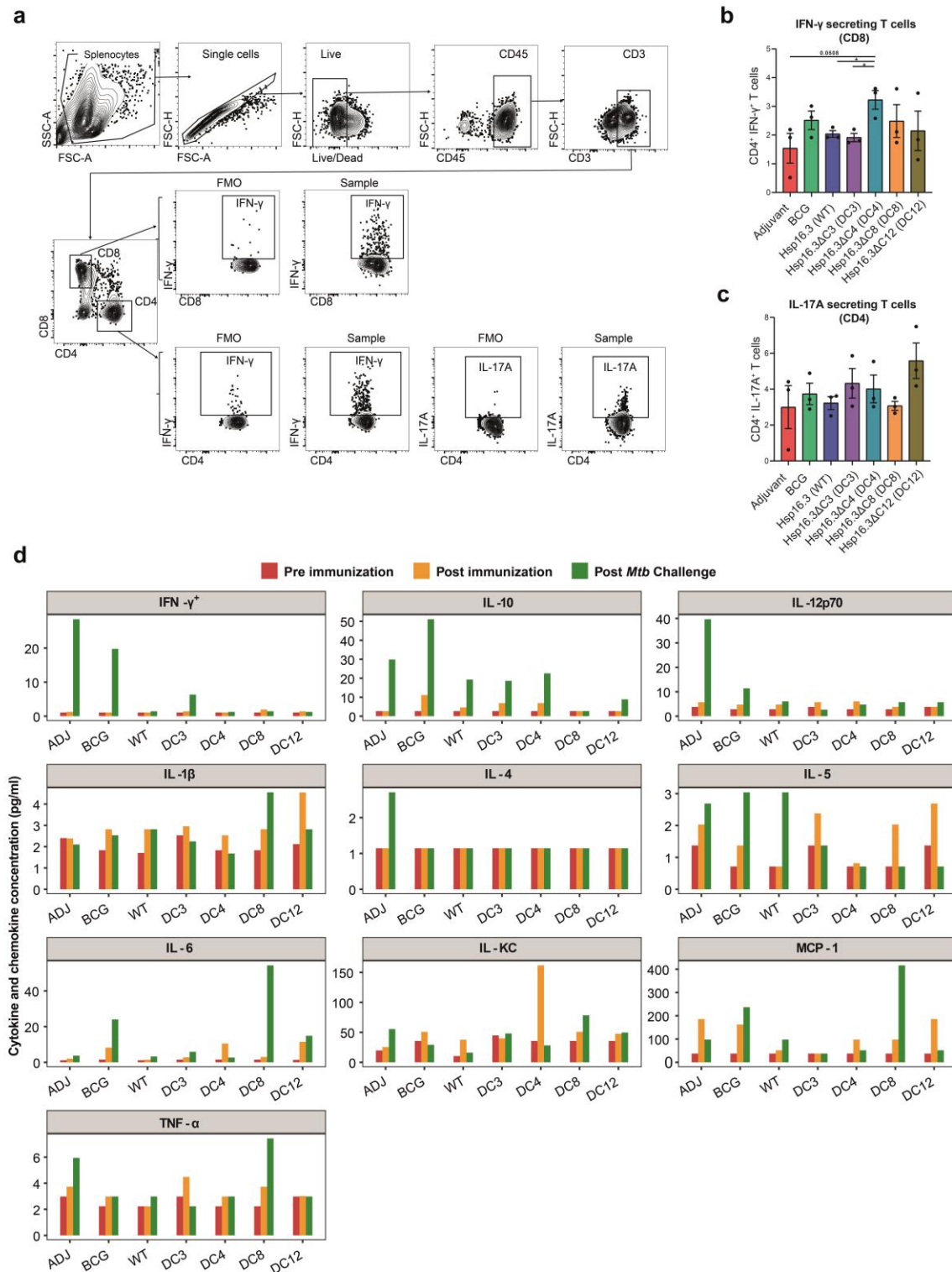
For the overexpression and purification of wild-type and C-terminal region-truncated mutants, firstly, the expression plasmids pET28b- Hsp16.3WT, pET28b- Hsp16.3ΔC3, pET28b-Hsp16.3ΔC4, pET28b-Hsp16.3ΔC8, and pET28b-Hsp16.3ΔC12 were transformed into *E. coli* BL21 (DE3) cells, individually. The detailed procedures of overexpression and purification are mentioned here sequentially.

At first, 5 ml of overnight *E. coli* BL21(DE3) bacterial cultures (containing these expression plasmids), were inoculated into respective 250 ml of freshly prepared Luria Bertani broth medium (HIMEDIA, M575) supplemented with kanamycin (50 mg/ml; Sisco Research Laboratories, 99311) individually and incubated at 37°C, 250 rpm, till the OD at 600 nm had reached 0.5-0.7. Then, the induction of these proteins was executed by adding isopropyl thio-β-D-galactoside (IPTG) (Sisco Research Laboratories, 67208), which maintained a final concentration of 0.4 mM. After induction, the bacterial cultures were incubated for an additional 6 to 7 h at 37°C. Then these cells were obtained by centrifugation at $5000 \times g$ for 10 min at 4°C.

For execution of purification, firstly, the bacterial cell pellets were resuspended in lysis buffer (5 ml/g), containing 50 mM NaH₂PO₄ (Sisco Research Laboratories, 59443), 300 mM NaCl (Sisco Research Laboratories, 1940103), 10 mM imidazole (Sisco Research Laboratories, 61510), 1 mM PMSF (Sisco Research Laboratories, 87606), and 20 μg/ml DNase (Sigma-Aldrich, D4138-80 KU) at pH 8.0. After the addition of this buffer to cell pellets, the pellets were gently mixed by flushing at 30-minute intervals for 4 h on ice. Then the cell lysates were immersed in ice, and by using a digital probe sonicator, the cells were dispersed by sonication of six on/off cycles (6 × 60 s bursts at 38% amplitude). The sonicated samples were centrifuged at $10000 \times g$ for 60 min at 4°C. These proteins were obtained in the soluble fraction. After centrifugation, the lysates were then kept for binding with gentle mixing for ~1 h at room temperature with an appropriate amount of Ni-NTA resin according to the instructions of the manufacturer (Qiagen, 30210, Chatsworth, CA, USA) before loading onto a prepared column. The polypropylene columns were washed previously with buffer containing 50 mM NaH₂PO₄, 300 mM NaCl, and 10 mM imidazole at pH 8.0. The required proteins were eluted from these columns with the same buffer containing different concentrations of imidazole (100 mM, 250 mM, and 500 mM). The purified 250 mM fractions were dialyzed for 3 h against 50 mM phosphate buffer (pH 7.5), followed by overnight dialysis against 50 mM phosphate buffer [NaH₂PO₄ (Sisco Research Laboratories, 59443), Na₂HPO₄ (Sisco Research Laboratories, 21669)] containing 10 mM imidazole at 4°C. Then, on the next day, the dialysed fractions containing these proteins with a 6X His-tag are subjected to thrombin cleavage procedure. Thrombin enzyme (Sisco Research Laboratories, RM5469) is used to cleave the 6X His-tag from all these proteins. We have kept the reaction mixture (1 ml) as 1 mg of the protein with 6X His-tag and thrombin of 10 NIH units, in 50 mM phosphate buffer containing 10 mM imidazole (pH 7.5). This reaction mixture was incubated for 18 h at 20°C, in order to execute the complete thrombin cleavage procedure. After this process was over, all the reaction mixtures were then passed through an appropriate amount of pre-equilibrated (with 50 mM phosphate buffer containing 10 mM imidazole, pH 7.5) p-benzamidine agarose resin (Sigma Chemical Co., A7155, St Louis, MO, USA), in order to remove the thrombin. The obtained solutions of proteins contain both 6X His-tag (uncut) and 6X His-tag (cut) proteins. Then these solutions were kept for binding with gentle mixing for ~1 h at

room temperature for the binding of the uncut protein to Ni-NTA resin. Then, these Ni-NTA resins were loaded onto respective empty polypropylene columns, and the collected eluents contained the required thrombin cut (devoid of 6X His-tag) proteins. The eluents which does not have the 6X His-tag were dialyzed extensively against 50 mM phosphate buffer (pH 7.5) at 4°C. After the dialysis was over, we stored the proteins at -20°C. Then, SDS-PAGE (15%) was run to assess the purity of these proteins. The concentration of these purified proteins was determined by using the UV-visible spectroscopic method. These proteins are devoid of any tryptophan residue; thus, by measuring the absorbance at 278 nm (due to the presence of tyrosine residue) and by using the extinction coefficients obtained from the Expasy Protparam software using the amino acid sequence of these proteins, the concentration was determined¹.

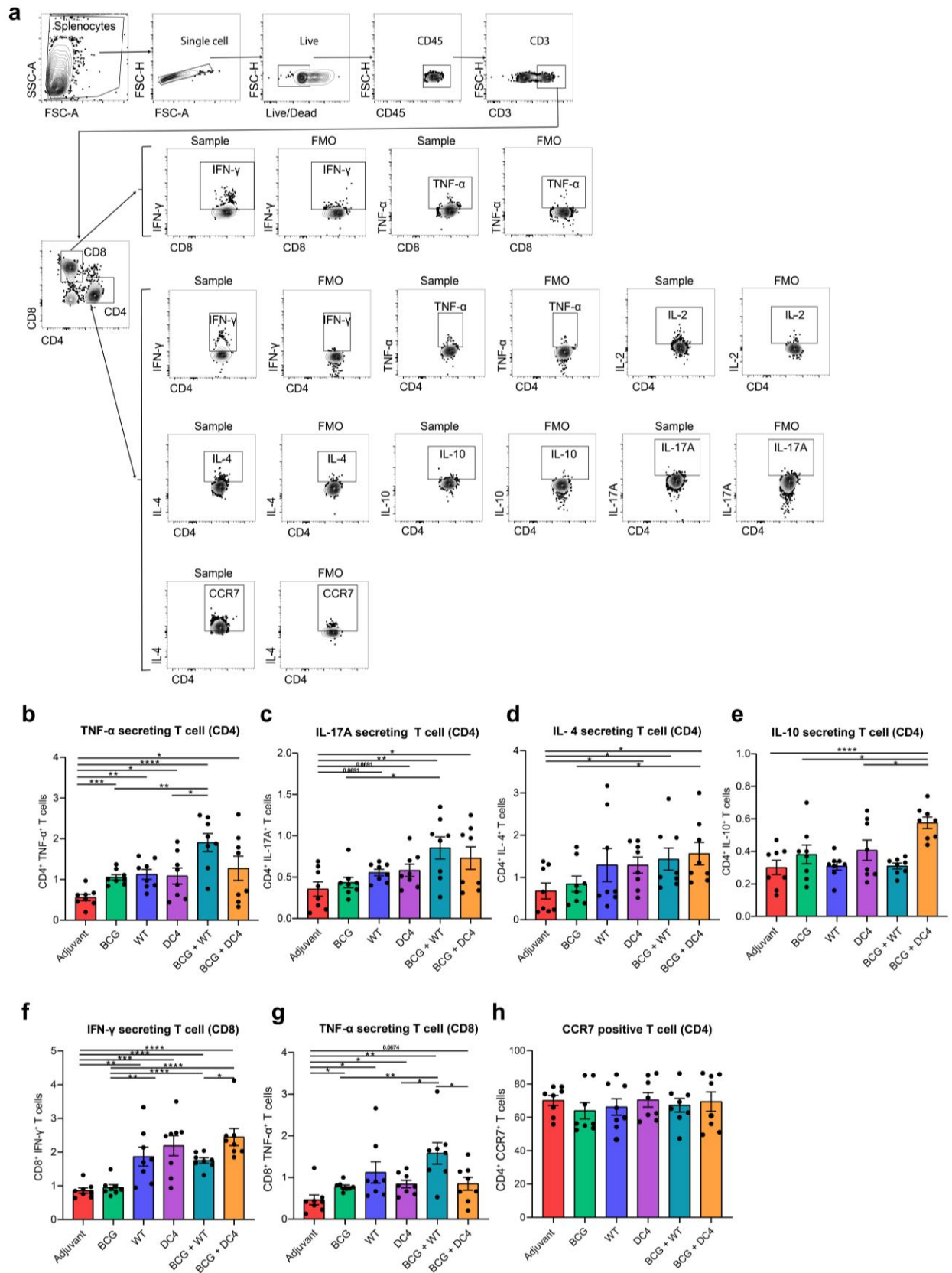
Supplementary Fig. 1: Gating strategy and evaluation of intracellular cytokines in spleens of adjuvant-, or BCG-, or Hsp16.3-, or Hsp16.3- variant-immunized mice.



(a) Single cell suspension was prepared from the spleen harvested from mice at 6 weeks post-immunization. 0.5 million cells were seeded in a 96-well plate and stimulated with respective antigens (40 μ g/ml) for 24 h to determine intracellular cytokine levels. Subsequently, cells were stained with surface and intracellular cytokines as described in methods section. The data was acquired on Cytex Aurora and analyzed using FlowJo software.

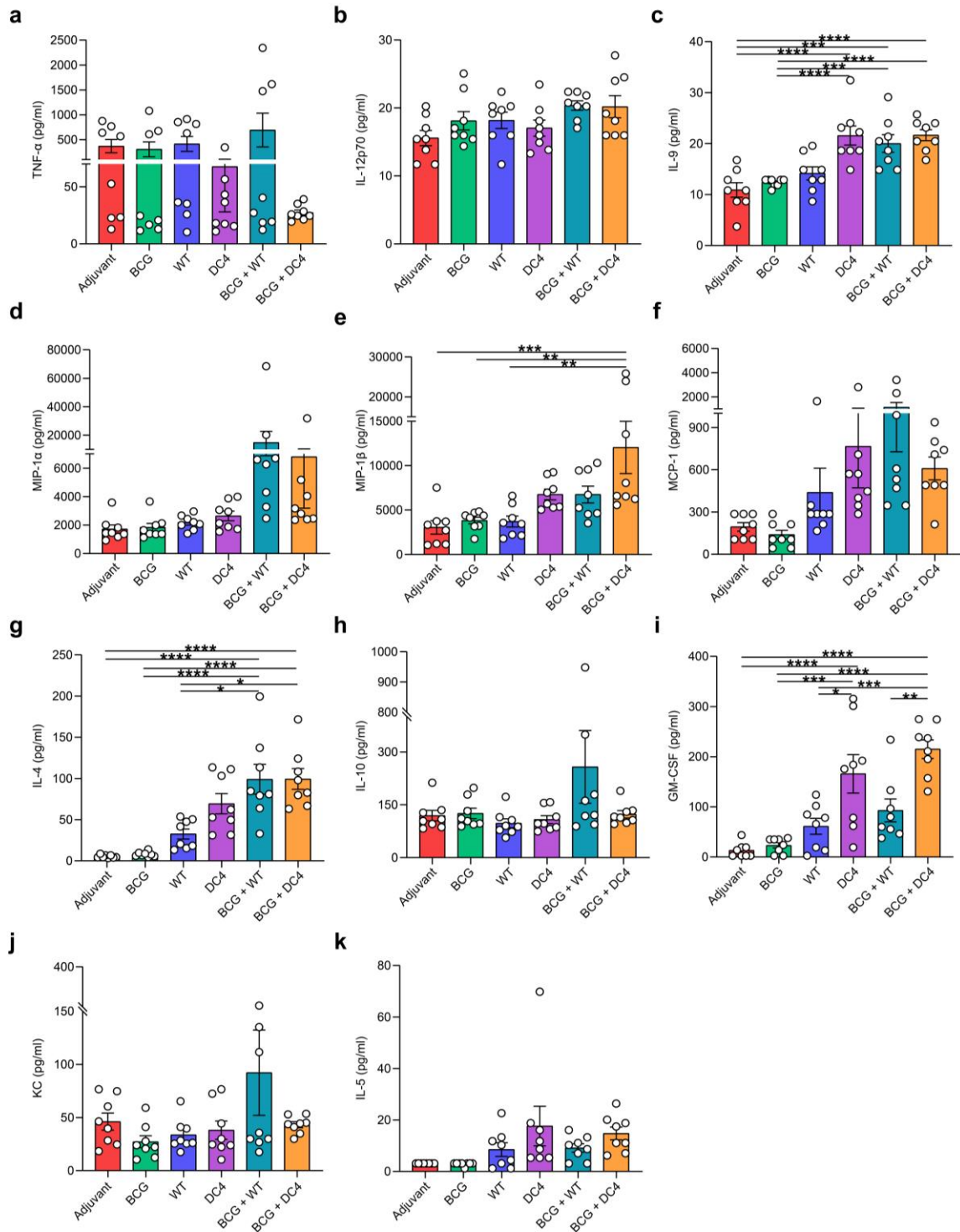
The gating strategy was followed in a sequential manner (left to right), as shown in the FACS contour plots above. IFN- γ ⁺ and IL-17A⁺ cells were gated on CD4⁺ T cells or CD8⁺ T cells as indicated above. **(b-c)** Bar graphs showing percentage frequency mean \pm SEM of CD8⁺ IFN- γ ⁺ T cells **(b)** and CD4⁺ IL-17A⁺ T cells **(c)** are obtained from 3 animals from a single experiment. P-values depicted on the graphs were assessed using one-way ANOVA. Source Data is provided as a Source Data file. **(d)** Demonstrating the level of cytokines in serum at 0 (pre-immunization), 6 (post-immunization), and 11 weeks (post-challenge) time points [For samples in which cytokine concentrations were below the lower limit of quantification (LLOQ) as defined by the assay, a value equal to one-half of the LLOQ was imputed for subsequent analyses].

Supplementary Fig. 2: Gating strategy and evaluation of intracellular cytokines in spleens of adjuvant-, BCG-, or WT-, or DC4-, or BCG + WT-, or BCG + DC4- immunized mice.



(a) Single cell suspension was prepared from the spleen harvested from mice at 6 weeks post-immunization. 0.5 million cells were seeded in a 96-well plate and stimulated with respective antigens (40 $\mu\text{g/ml}$) for 24 h to determine intracellular cytokine levels. Subsequently, cells were stained with surface and intracellular cytokines as described in methods section. The data was acquired on Cytex Aurora and analyzed using FlowJo software. The gating strategy was followed in a sequential manner (left to right), as shown in the FACS contour plots above. $\text{IFN-}\gamma^+$, $\text{TNF-}\alpha^+$, IL-2^+ , IL-17A^+ , IL-4^+ , IL-10^+ , and CCR7^+ cells were gated on CD4^+ T cells or CD8^+ T cells as indicated above. **(b-h)** Bar graphs showing the percentage frequency mean \pm SEM of CD4^+ $\text{TNF-}\alpha^+$ T cells **(b)**, CD4^+ IL-17A^+ T cells **(c)**, CD4^+ IL-4^+ T cells **(d)**, CD4^+ IL-10^+ T cells **(e)**, CD8^+ $\text{IFN-}\gamma^+$ T cells **(f)**, CD8^+ $\text{TNF-}\alpha^+$ T cells **(g)**, and CD4^+ CCR7^+ T cells **(h)** were obtained from 8 animals from two separate experiments. P-values depicted on the graphs were assessed using one-way ANOVA. Source data are provided as a source data file.

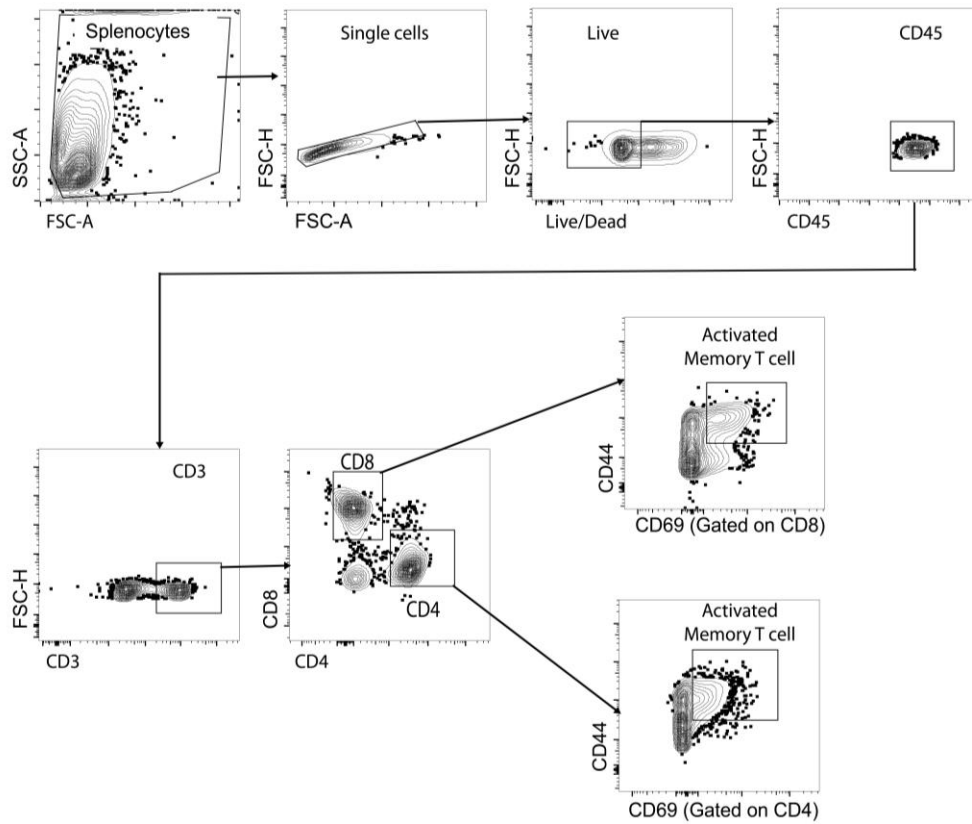
Supplementary Fig. 3: Bar graph depicting the different cytokine and chemokine levels in the culture supernatants of stimulated splenocytes.



(a-k) Single-cell suspensions were prepared from spleens harvested at 6 weeks post-immunization. 0.5 million cells were cultured in 96-well plates and stimulated with the respective antigens (40 μ g/ml) for 24 h. Culture supernatants were collected, and cytokine and chemokine levels were quantified using Bio-Plex. Bar graphs depicting mean \pm SEM of secretory levels of TNF- α (a), IL-12p70 (b), IL-9 (c), MIP-1 α (d), MIP-1 β (e), MCP-1 (f), IL-4 (g), IL-10 (h), GM-CSF (i), KC (j), and IL-5 (k). For samples in which cytokine concentrations were

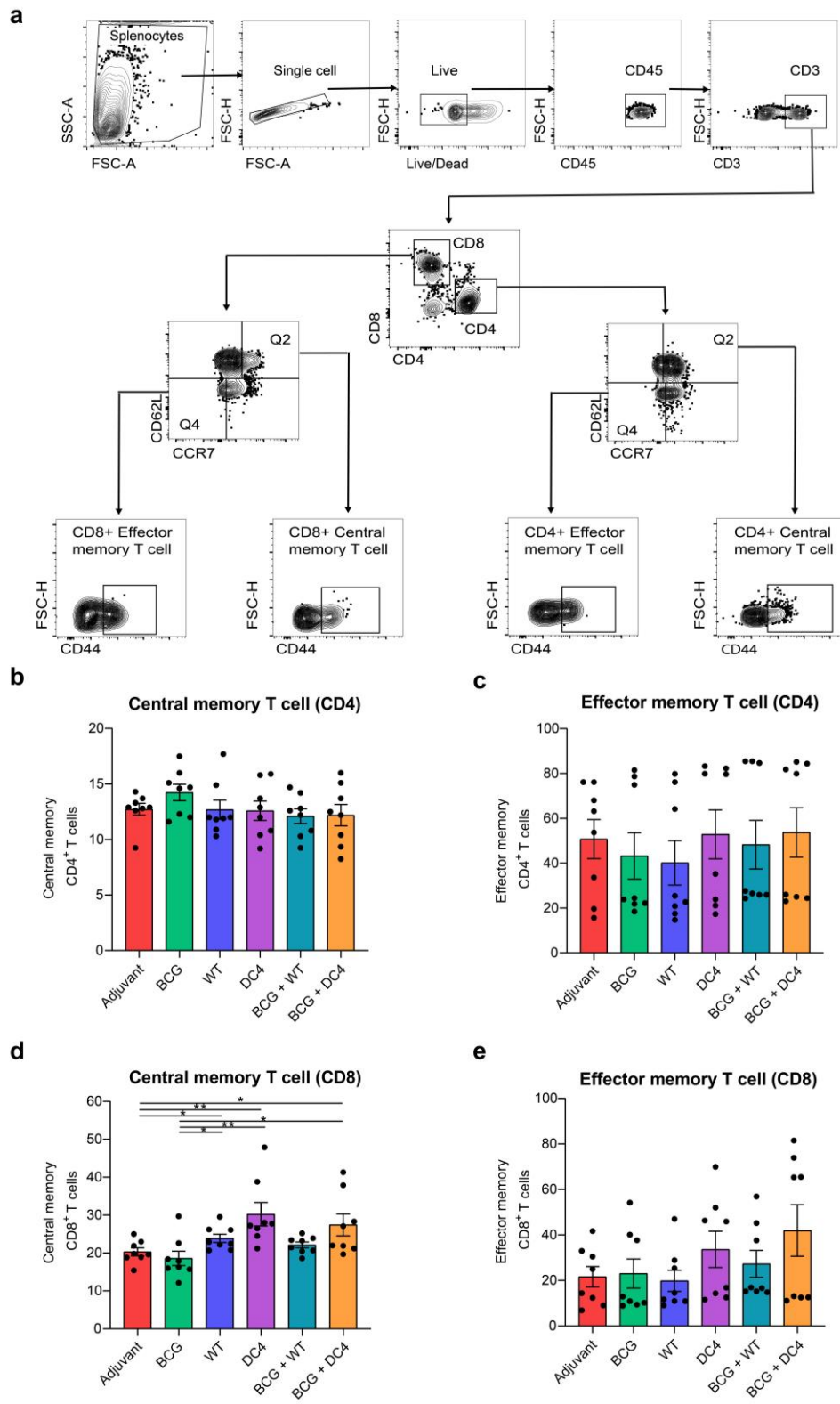
below the lower limit of quantification (LLOQ) as defined by the assay, a value equal to one-half of the LLOQ was imputed for subsequent analyses. P-values depicted on the graphs were assessed using one-way ANOVA. Source data are provided as a source data file.

Supplementary Fig. 4: Gating strategy for the measurement of activated memory T-cell responses in spleens of adjuvant-, BCG-, or WT-, or DC4-, or BCG + WT-, or BCG + DC4- immunized mice.



Single-cell suspension was prepared from the spleens of immunized mice at 6 weeks post-immunization. The cells were seeded in a 96-well plate and surface-stained as described in the methods section. The data was acquired on Cytex Aurora and analyzed using FlowJo software. The gating strategy was followed in a sequential manner (left to right) as shown in the FACS contour plots above. Activated memory T cells were gated on CD4⁺ or CD8⁺ T cells as indicated above.

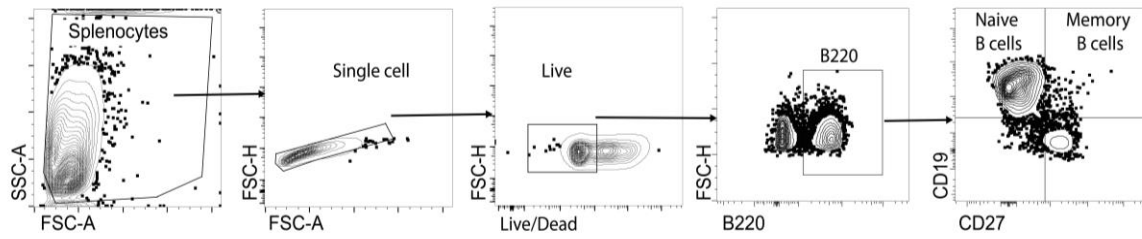
Supplementary Fig. 5: Gating strategy and evaluation of memory T cell responses in spleens of adjuvant-, or BCG-, or WT-, or DC4-, or BCG + WT-, or BCG + DC4- immunized mice.



(a) Single-cell suspension was prepared from the spleens of immunized mice at 6 weeks post-immunization. The cells were seeded in a 96-well plate and surface-stained as described in the methods section. The data was

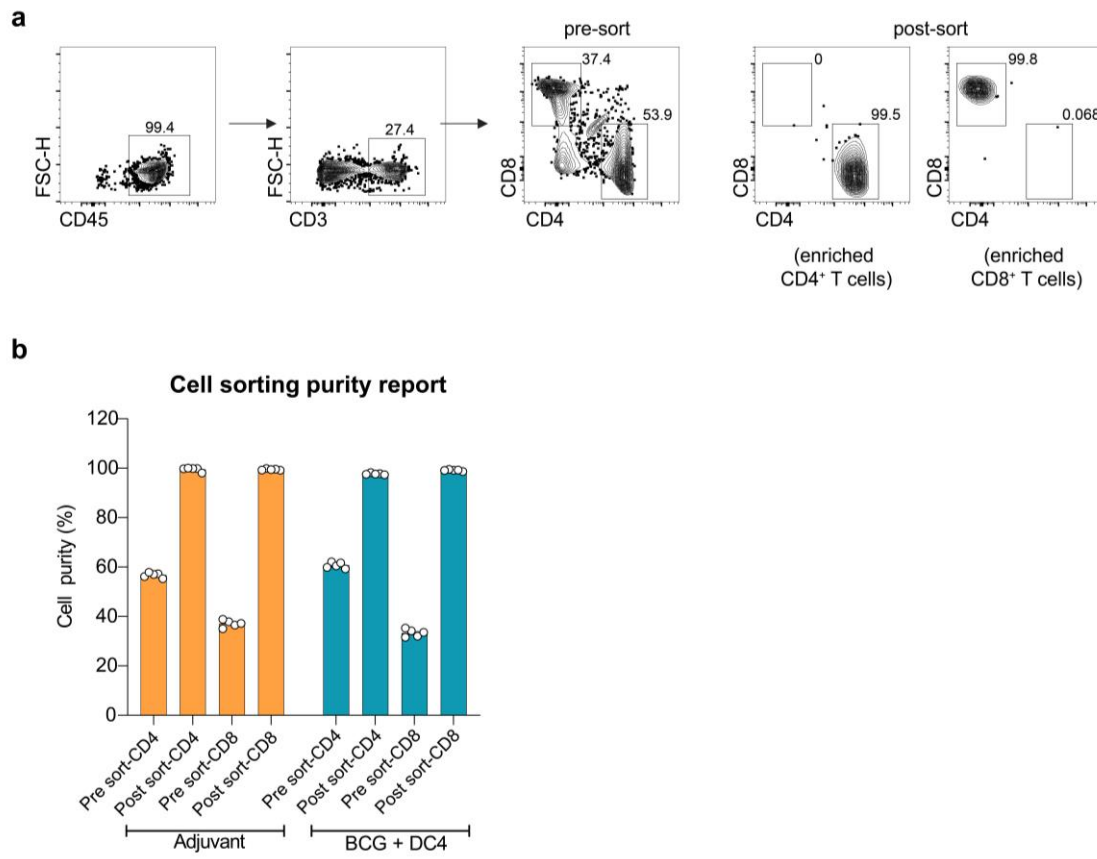
acquired on Cytex Aurora and analyzed using FlowJo software. The gating strategy was followed in a sequential manner (left to right) as shown in the FACS contour plots above. Central and effector memory T cells were gated on CD4⁺ or CD8⁺ T cells as indicated above. **(b-e)** Representative FACS plots showing the frequency of central and effector memory CD4⁺ Th cells and CD8⁺ Tc cells in spleens of adjuvant-, or BCG-, or WT-, or DC4-, or BCG + WT-, or BCG + DC4- immunized mice. These panels show the proportion of central memory CD4⁺ Th cells **(b)**, effector memory CD4⁺ Th cells **(c)**, central memory CD8⁺ Tc cells **(d)**, effector CD8⁺ Tc cells **(e)** in the spleens of adjuvant-, or BCG-, or WT-, or DC4-, or BCG + WT- or BCG + DC4- immunized mice. The data shown in these panels are the mean \pm SEM of the proportion of cells obtained from 8 animals across two independent experiments. P-values depicted on the graphs were assessed using one-way ANOVA. Source data are provided as a source data file.

Supplementary Fig. 6: Gating strategy for the measurement of memory B cells in spleens of adjuvant-, or BCG-, or WT-, or DC4-, or BCG + WT-, or BCG + DC4- immunized mice.



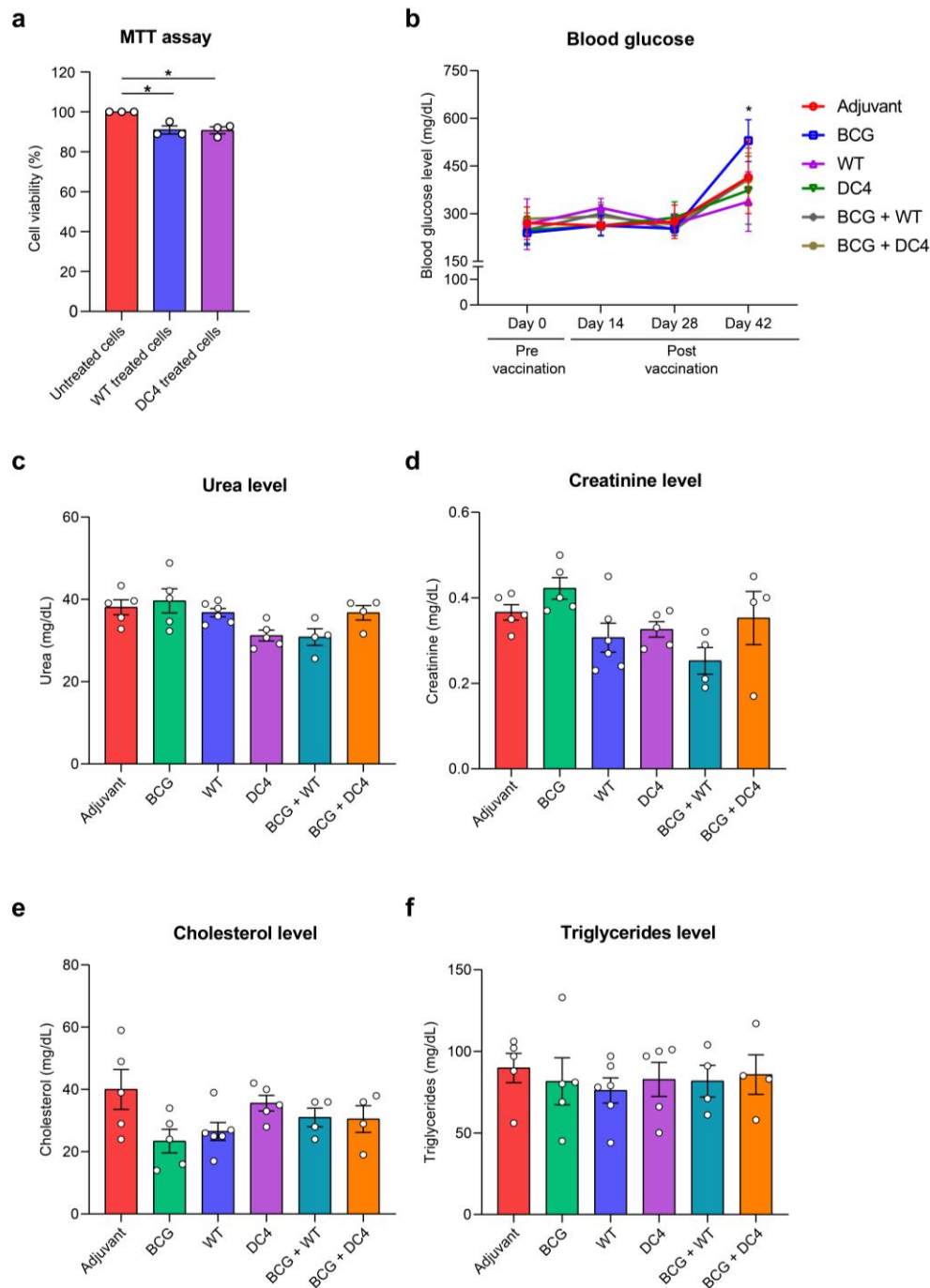
Single-cell suspension was prepared from the spleens of immunized mice at 6 weeks post-immunization. 0.5 million cells were seeded in a 96-well plate and surface-stained as described in the methods section. The data was acquired on Cytex Aurora and analyzed using FlowJo software. The gating strategy was followed in a sequential manner (left to right) as shown in the FACS contour plots above. Memory B cells were gated on B220 B cells as indicated above.

Supplementary Fig. 7: Purity assessment of sorted cells used for adoptive transfer.



(a) Representative flow cytometry contour plots of purified CD4⁺ and CD8⁺ T cells (post-sort) from vaccinated (adjuvant and BCG + DC4) mice splenocytes (pre-sort) used for adoptive transfer. **(b)** The bar graph illustrates the sorting purity of CD4⁺ and CD8⁺ T cells isolated from splenocytes of adjuvant- and BCG + DC4- vaccinated mice.

Supplementary Fig. 8: *Ex vivo* and *in vivo* toxicological assessment of vaccine candidates.



(a) Cell viability of THP-1-derived macrophages exposed to 40 μ g/ml subunit vaccine candidates Hsp16.3 (WT) and Hsp16.3 Δ C4 (DC4) for 24 h using MTT assay. (n=3) **(b)** Blood glucose levels were measured to evaluate metabolic stability. (n=6) **(c)** Kidney function parameters like serum urea levels were quantified in all the vaccinated mice group post vaccination to assess potential nephrotoxicity. (n=4 to 6) **(d)** Kidney function parameters, like serum creatinine levels, were quantified in all the vaccinated mice group post vaccination to assess potential nephrotoxicity. (n=4 to 6) **(e)** Lipid profile analysis, such as serum total cholesterol levels, was quantified in all the vaccinated mice groups post vaccination to monitor any alterations in lipid metabolism.

(n=4 to 6) (f) Lipid profile analysis, such as serum total triglyceride levels, was quantified in all the vaccinated mice groups post vaccination to monitor any alterations in lipid metabolism. (n=4 to 6) Level of significance for comparison between different samples was determined using one-way ANOVA. Differences with * $p < 0.05$, ** $p < 0.01$, *** $p < 0.001$, or **** $p < 0.0001$ were considered statistically significant.

References

- 1 Panda AK, Chakraborty A, Nandi SK, Kaushik A, Biswas A. The C-terminal extension of Mycobacterium tuberculosis Hsp16.3 regulates its oligomerization, subunit exchange dynamics and chaperone function. *FEBS J* 2017; **284**: 277–300.